Two-Dimensional Phase Transition Mediated by Extrinsic Defects

A. V. Melechko, J. Braun, H. H. Weitering, and E. W. Plummer
Department of Physics and Astronomy, The University of Tennessee, Knoxville, Tennessee 37996
and Solid State Division, Oak Ridge National Laboratory, Oak Ridge, Tennessee 37831
(Received 22 February 1999)

We have investigated the $(\sqrt{3} \times \sqrt{3})$ to (3×3) phase transition in the α phase of Sn/Ge(111) with variable temperature STM at temperatures between 30 and 300 K. Point defects in the Sn film stabilize localized regions of the (3×3) phase, where the size is characterized by a temperature dependent length (exponential attenuation). The inverse of the attenuation length is a linear function of temperature showing that the phase transition occurs at 70 K. At low temperature a density wave mediated defect-defect interaction realigns the defects to be in registry with the (3×3) domains.

PACS numbers: 68.35.Rh, 68.35.Bs, 71.45.Lr, 72.10.Fk

Structural phase transitions belong to a group of phenomena, which are strongly related to surface symmetry and its lowering. In many cases a prediction of the order and universality class of an anticipated phase transition can be made based solely on the knowledge of the space group of the surface or adsorbate structure [1]. This idealized picture is rarely achieved in the real world, where defects and imperfections in the surface break the symmetry. Various types of surface phase transitions have been reported in the literature [2,3], and even though an atomistic picture of the phase nucleation process has remained elusive, it is generally believed that this process involves defects and impurities [4,5]. Since the energy differences between different phases on a surface are usually very small, a slight perturbation of this energy balance, coupled with the broken symmetry induced by an imperfection, can affect not only the transition temperature but also the temperature dependence of the order parameters near the critical point. For example, consider a system with a charge density wave (CDW) instability. Electrons in the normal state will screen charged impurities, producing an attenuated CDW or Friedel oscillation near the impurity sites. The ion cores follow the local charge rearrangement and, consequently, the normal-state symmetry is broken locally and short-range CDW order develops. The electronic response to the external perturbation [6], $\chi(\boldsymbol{q}, T)$, depends on the temperature, leading to the intriguing proposition that defects will in general affect the evolution of long-range ordering. Tosatti and Anderson concluded that "a CDW can be regarded as unattenuated Friedel oscillations" [7].

There is indeed evidence that imperfections have a strong influence on surface phase transitions. For example, the anticipated second-order phase transition on a Si(100) surface from a (2×1) to a $c(4 \times 2)$ structure is not sharp [8]. This behavior was qualitatively reproduced by Monte Carlo simulations based on an Ising spin model [9,10], in which the intrinsic dimer defect concentration (1%) on the surface was taken into account. Interestingly, a system consisting of the ideal Si(100) surface and defects is equivalent to an Ising spin system with a random magnetic field [9]. It has been speculated that the presence of defects blocks the basic atomic mechanism (a flip-flop motion of buckled dimers) responsible for the observed broadening of the phase transition on Si(100) [4].

We have chosen the recently discovered charge ordering transition in the α phase of Sn on Ge(111) [11–17] to study the interplay between a phase transition and defects. One-third of a monolayer of Sn forms a metastable $(\sqrt{3} \times \sqrt{3})$ overlayer on this surface at room temperature (RT). Upon cooling the surface, a phase transition to a (3×3) symmetry has been reported to occur at 210 K, as determined from LEED intensity measurements [11]. At RT, all Sn atoms appear identical (in the absence of defects) in the STM images, whereas at low temperature (LT) the filled state and empty state images show complimentary structures with a (3×3) symmetry. The bright atoms in the empty state images form a honeycomb structure with two bright spots per unit cell, while the bright atoms in the filled state image form a hexagonal structure with one bright atom per unit cell [11]. Ge substitutional defects (called Ge defects throughout this paper) have been identified to be the most common type of (point) defects in the Sn film [11,18]. A group of such defects surrounded by a (3×3) pattern is present in the left part of the filled state STM image in Fig. 1 which was recorded at $T = 120$ K, a temperature 90 K below the reported transition temperature. The (3×3) structure induced by the defects vanishes only a few unit cells away from the defects and the right side of the image consists solely of unreconstructed $(\sqrt{3} \times \sqrt{3})$ as in the RT images. It is obvious that the $\sqrt{3} \times \sqrt{3}$ to (3×3) phase transition has not yet occurred at 120 K. This study will demonstrate that the phase transition is at 70 K, about 140 K below the reported transition temperature.

In this Letter we report a real space study of the influence of extrinsic and intrinsic defects on a two-dimensional phase transition. It will be demonstrated that attenuated density waves with (3×3) symmetry originate from defects as shown in Fig. 1. The extent of these (3×3) waves is described by an exponential damping with a decay length $l(T)$. *The inverse decay length is*

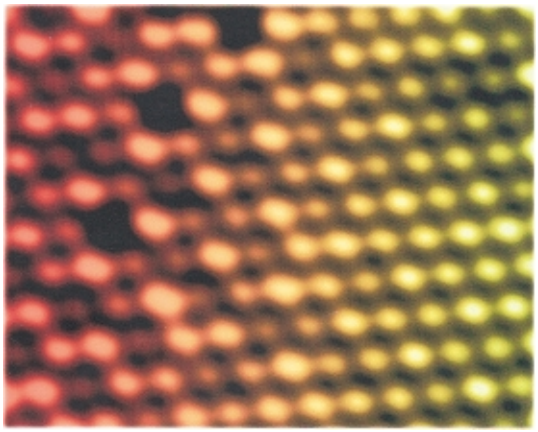

FIG. 1 (color). 119×66 Å^2 filled state constant current STM image ($V_{\text{sample}} = -1$ V, $I = 0.1$ nA) recorded at $T = 120$ K. The left portion of the image includes three Ge substitutional atoms (Ge defects). The system responds to this perturbation with a local (3×3) reconstruction around the defects which vanishes in the right part of the image.

linear with temperature, extrapolating to zero at 70 K, which we propose to be the transition temperature. At low temperatures, below the phase transition this model fails to explain the morphology of the surface, and, in particular, does not address the formation of sharp domain boundaries. Most striking is the observation that at low temperature there is a collective interaction between the density waves and the defects, moving the latter into alignment with the new (3×3) phase (in each domain).

The experiments were performed using a UHV omicron variable temperature STM that provided atomic resolution in a range of temperatures from 30 to 300 K. The temperatures were stabilized within 0.1 K and absolute temperatures were reproducible to within 5 K. Clean, well-ordered Ge(111) substrates were prepared by repeated Ne ion bombardment (1 kV) and annealing to 800 K until a sharp $c(2 \times 8)$ LEED pattern was observed. The α phase of Sn/Ge(111) $(\sqrt{3} \times \sqrt{3})$ was obtained by depositing $\frac{1}{3}$ of a monolayer of Sn at room temperature and then annealing to 500 K. The resultant surfaces consisted of $(\sqrt{3} \times \sqrt{3})$ reconstructed terraces with an average width of around 2000 Å. A reproducible average density of about 6.25×10^{-4} point defects per Å^2 (Ge substitutional defects and vacancies) was found in the Sn overlayers [see Fig. 2(a)]. This is consistent with previous reports [11,18]. Point defects appear as black spots in the filled state images surrounded by bright rings of nearest neighbor (NN) Sn atoms for Ge substitutional defects and by dark rings of NNs for vacancies [18,19]. In the empty state images Ge defects are brighter than vacancies. The majority of the defects were Ge substitutional atoms, 10 to 1 compared to vacancies.

The left panels of Fig. 2 show filled state STM images acquired in the constant current mode at three temperatures, (a) 295 (RT), (b) 165, and (c) 55 K. At RT the

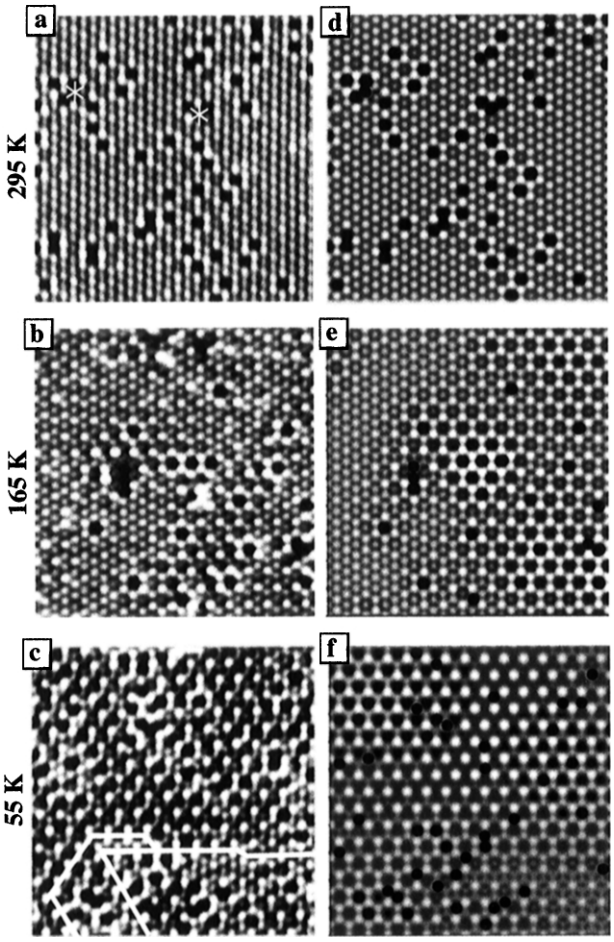

FIG. 2. 175×182 Å^2 filled state constant current STM images ($V_{\text{sample}} = -1$ V, $I = 0.1$ nA): (a) $T = 295$ K (RT); (b) $T = 165$ K. The two sole vacancies in the image are labeled by white asterisks. (3×3) reconstructed patches are visible in the vicinity of the defects. (c) $T = 55$ K; the white lines indicate sharp domain boundaries. (d)–(f): Numerically simulated images [Eq. (1)] using the defect positions (marked by black circles) deduced from images (a)–(c), respectively. Different decay lengths, l, were used to obtain agreement with the data: (d) $l = 11$ Å; (e) $l = 25$ Å; (f) $l = 100$ Å.

$(\sqrt{3} \times \sqrt{3})$ structure is perturbed only in the immediate vicinity of a defect. When the temperature is lowered, the range of the (3×3) perturbation produced by the defects increases, as can be seen in Fig. 1 for 120 K or in Fig. 2(b) for 165 K. Again it should be pointed out that a phase transition has not occurred in either of these figures. In contrast, Fig. 2(c) shows an example of a completely reconstructed (3×3) Sn layer at $T = 55$ K, where the white line highlights the existence of a sharp domain wall between different orientations of the (3×3) phase. From this data we can conclude that the transition temperature is between 120 and 55 K, significantly lower than the reported 210 K [11].

Visual inspection of STM images suggested to us that the charge rearrangement is the result of the superposition of patterns induced by each defect. To confirm this

observation we have carried out a numerical simulation of the filled state STM images. The trial function included the existing $\sqrt{3} \times \sqrt{3}$ periodicity [$f_{\sqrt{3}\times\sqrt{3}}(r)$] modulated by the sum of three exponentially damped cosine waves with a periodicity of a 3×3 lattice originating at each defect. The exponential decay was characterized by a length parameter $l(T)$,

$$I(\mathbf{r}) = f_{\sqrt{3}\times\sqrt{3}}(\mathbf{r}) + \sum_{n}^{N} A_n e^{\frac{-|\mathbf{r}-\mathbf{r}_n|}{l(T)}} \sum_{i}^{3} \cos[\mathbf{k}_i(\mathbf{r} - \mathbf{r}_n) + \phi_n]. \quad (1)$$

The experimental images were simulated by summing over the number of defects N in the image. The amplitude of the density wave, A_n, is a constant so that only the phase ϕ, and the decay length $l(T)$ are parameters. Vacancies and defects are modeled by phases $\phi_n = 0$ and $\phi_n = \pi$, respectively. The three images on the right of Fig. 2 best reproduce the experimental data with $l(T)$ as the only parameter. Simulations were also carried out for images recorded at 120 K (Fig. 1). The best agreement between experimental data for RT, 165 and 120 K and the simulated images was achieved by inverse length parameters $1/l(T)$ collected in Fig. 3(a). The data for $T = 55$ K [Fig. 2(c)] could not be fitted; the consequence of this will be discussed later.

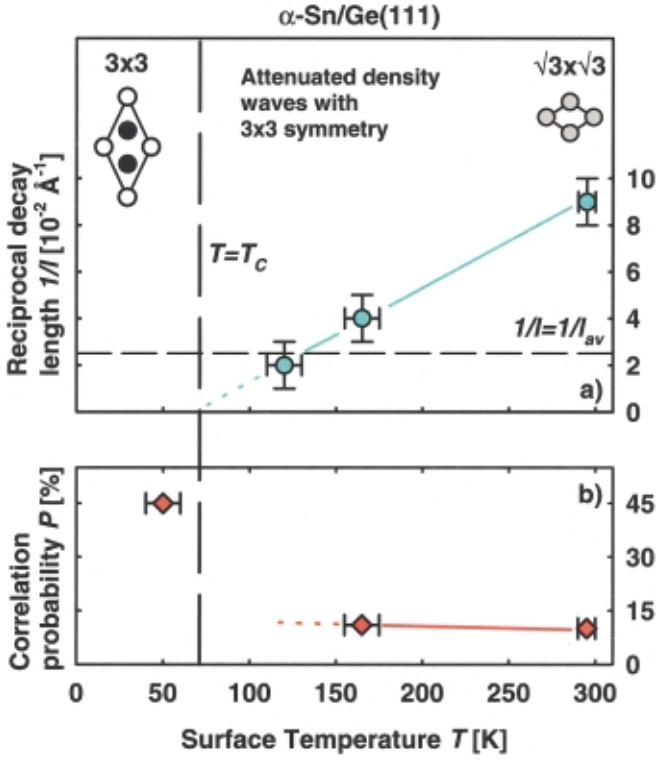

FIG. 3 (color). (a) Temperature dependence of the reciprocal decay length $1/l(T)$ [Eq. (1)]. The phase transition temperature is $T_c \approx 70$ K indicated by a vertical dashed line. A ($\sqrt{3} \times \sqrt{3}$) unit cell is shown in the upper right part of the figure. The upper left inset shows a (3×3) unit cell. In the text, we refer to the open and black circles as corner atoms and inner sites, respectively. (b) Temperature dependence of the probability to find a correlated sampling area in STM images (see text).

Figure 3 clearly shows that the inverse length parameter $1/l(T)$ is a monotonic function of temperature, extrapolating to zero at approximately 70 K. At this point the decay length becomes infinity. This singularity defines the phase transition temperature of the system, $T_c \approx 70$ K. *This technique to determine the phase transition temperature T_c is not restricted to the Sn/Ge(111) system studied here and can be used on any similar system.*

It was not possible to simulate the experimental images taken at low temperature using Eq. (1) [compare Figs. 2(c) and 2(f) ($T = 55$ K)]. *It is impossible to reproduce the sharp domain walls shown in Fig. 4 for $T = 30$ K*, the domain size observed in the images, or the fundamental symmetry of the image. A Ge substitutional defect would produce a honeycomb 3×3 structure when $l(T) \rightarrow \infty$, but what is seen is the hexagonal structure. Obviously, Eq. (1) is not appropriate for the LT phase.

The LT STM images show (3×3) domains of average size 100×100 Å^2. This size agrees well with (3×3) domain diameters determined by x-ray diffraction, (90 ± 20) Å [12]. Visual inspection of these images revealed that almost all (90%) of the Ge substitutional defects within a single domain had aligned themselves to be in registry with that domain, that is they always replace a dark Sn atom. Ge defects very rarely replace the bright atoms in LT STM images. In contrast Ge defects at RT appear to be randomly distributed in the images. The inset in Fig. 3 shows the options available for a Ge defect in the (3×3) unit cell. There are three atoms in the unit cell and in principle three different options for the Ge defect, but the STM images [11,18] and structural analysis [12] show that two of the sites are equivalent (dark inside atoms).

A statistical analysis of STM images recorded at 295, 165, and 55 K was performed in the following fashion [20]. A *sampling area* (SA) slightly smaller (80×80 Å^2) than the average (3×3) domain size was chosen.

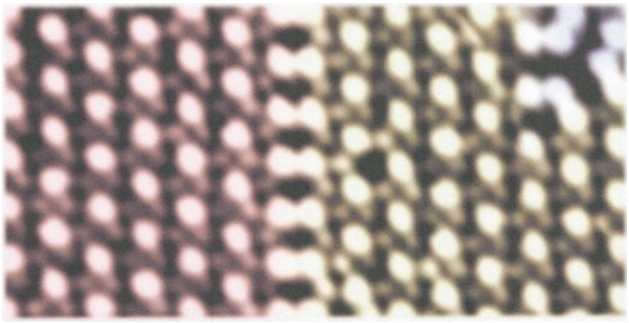

FIG. 4 (color). 140×42 Å^2 filled state constant current STM image ($V_{\text{sample}} = -1$ V, $I = 0.1$ nA) recorded at $T = 30$ K. The image shows three different (3×3) domains separated by sharp domain boundaries.

The surface was then randomly sampled with these SAs. We define a SA *correlated* if all the defects are located on sites of the dark inside atoms (see inset of Fig. 3) of its (3×3) cells. The probability P of finding a correlated SA in a STM image was determined from the ratio of the number of correlated SAs to the total number of SAs selected (typically 250 SAs per STM image). At LT, about 45% of all SAs were correlated. If we were to place all SAs within a single domain, then the probability P would be 95%. The LT probability of 45% just reflects the many times that the SA lies over two or more (3×3) domains. P changes dramatically if we apply the same counting procedure to RT STM images. Only 10% of all SAs were correlated at RT and $T = 165$ K. This 10% probability of finding correlated SAs is consistent with an analysis of computer generated STM images, where all defects were randomly distributed. The temperature dependence of P in Fig. 3(b) shows the dramatically higher correlation in the LT images. Data for a statistical analysis at other temperatures are currently not available.

We conclude that Ge defects are randomly distributed for temperatures as low as 165 K and spatially correlated on a length scale of about 100 Å [the average (3×3) domain size] at LT. The data set for the 120 K is not extensive enough to perform a statistical analysis. The transition from randomly distributed to correlated defects involves the *motion* of the defects. This observation suggests that the motion of defects is controlled by a defect-defect interaction, which sets in for $l \geq l_{\mathrm{av}}$, where l_{av} is the average NN distance between Ge defects, $l_{\mathrm{av}} = 45$ Å [horizontal dashed line in Fig. 3(a)]. We propose that *a density wave mediated defect-defect interaction drives the motion of Ge defects at LT.*

In conclusion, we have observed on an atomic scale the complex interplay between defects and a two-dimensional phase transition, which may impact the general picture of phase transitions in two dimensions. A perturbation of the charge rearrangement in the vicinity of defects already exists at room temperature. This distortion contains the symmetry of the (3×3) ground state of the system and grows exponentially in extent as the temperature is lowered showing clearly that the phase transition in the absence of defects is at $T = 70$ K not $T = 210$ K as previously reported. At low temperature a collective interaction between Ge substitutional defects and an ordering of the defects within each (3×3) domain is observed. This interaction is mediated by density waves. Ge defects can act in two contrasting ways. On one hand, they cause a *local* (3×3) reconstruction at temperatures well above the phase transition temperature of the system, $T_c = 70$ K. On the other hand, defects are distributed randomly on the surface at room temperature and actually *inhibit* the (3×3) reconstruction of the entire Sn film.

The *mobile* Ge substitutional defects cannot be treated as a given external field in a random field model [9,21]. They introduce a new dynamical variable which has a strong influence on the critical properties of the Sn/Ge(111) system.

We are indebted to K. Terakura for carefully reading the manuscript and W. W. Pai and R. Matzdorf for assistance in the initial stages of the experiment. J. B. thanks the German Research Society (DFG) for support. Primary funding was from the National Science Foundation under Grant No. DMR-9801830. H. H. W. was supported by NSF DMR-9705246. ORNL is managed by Lockheed Martin Energy Research Corp. for U.S. DOE under Contract No. DE-AC05-96OR22464.

[1] M. Schick, Prog. Surf. Sci. **11**, 245 (1981).
[2] A. Zangwill, *Physics at Surfaces* (Cambridge University Press, Cambridge, England, 1992).
[3] B. N. J. Persson, Surf. Sci. Rep. **15**, 4 (1992).
[4] K. Terakura, T. Yamasaki, and Y. Morikawa, Phase Trans. **53**, 143 (1994).
[5] H. Pfnür, C. Voges, K. Budde, and L. Schwenger, Prog. Surf. Sci. **53**, 205 (1996).
[6] E. Tosatti, in *Electronic Surface and Interface States on Metallic Systems*, edited by E. Bertel and M. Donath (World Scientific, Singapore, 1995), p. 67.
[7] E. Tosatti and P. W. Anderson, Jpn. J. Appl. Phys. Suppl. **2**, 381 (1974).
[8] T. Tabata, T. Aruga, and Y. Murata, Surf. Sci. **179**, L63 (1987).
[9] K. Inoue, Y. Morikawa, K. Terakura, and M. Nakayama, Phys. Rev. B **49**, 14 774 (1994).
[10] Y. Nakamura, H. Kawai, and M. Nakayama, Phys. Rev. B **55**, 10 549 (1997).
[11] J. M. Carpinelli, H. H. Weitering, M. Bartkowiak, R. Stumpf, and E. W. Plummer, Phys. Rev. Lett. **79**, 2859 (1997).
[12] J. Zhang, Ismail, P. J. Rous, A. P. Baddorf, and E. W. Plummer, Phys. Rev. B (to be published).
[13] J. M. Carpinelli, H. H. Weitering, E. W. Plummer, and R. Stumpf, Nature (London) **381**, 398 (1996).
[14] A. Goldoni and S. Modesti, Phys. Rev. Lett. **79**, 3266 (1997).
[15] R. I. G. Uhrberg and T. Balsubramanian, Phys. Rev. Lett. **81**, 2108 (1998).
[16] G. Le Vay, V. Yu. Aristov, O. Boström, J. M. Layet, M. C. Asensio, J. Avila, Y. Huttel, and A. Cricenti, Appl. Surf. Sci. **123/124**, 440 (1998).
[17] J. Avila, A. Mascaraque, E. G. Michel, M. C. Asensio, G. Le Lay, J. Ortega, R. Perez, and F. Flores, Phys. Rev. Lett. **82**, 442 (1999).
[18] H. H. Weitering, J. M. Carpinelli, A. V. Melechko, J. Zhang, M. Bartkowiak, and E. W. Plummer (to be published).
[19] J. M. Carpinelli, H. H. Weitering, and E. W. Plummer, Surf. Sci. **401**, L457 (1998).
[20] Details of the statistical analysis will be presented in a forthcoming paper.
[21] D. S. Fisher, G. M. Grinstein, and A. Khurana, Phys. Today **41**, No. 12, 56 (1988).